

Thin film flow over substrates with topography

P.H. Gaskell, Y.-Y. Koh, P.K. Jimack*, M. Sellier, H.M. Thompson and M.C.T. Wilson
Engineering Fluid Mechanics Research Group, School of Mechanical Engineering
*School of Computing

University of Leeds, Leeds, LS2 9JT, UK

Presented at the 12th International Coating Science and Technology Symposium
September 20-22, 2004 • Rochester, New York

ISCST shall not be responsible for statements or opinions contained in papers or printed in its publications.

This paper considers the particular case of gravity-driven flow down an inclined plane - as illustrated in figure 1 - of an evaporating thin liquid film, thickness $H(X, Y, T)$, composed of a resin dissolved in a volatile solvent, as it encounters well-defined topography, $S(X, Y)$. It builds on, extends and complements the recent experimental, Decré & Baret (2003), and theoretical analysis, Gaskell *et al.* (2004a), of the flow of thin water films over such substrates. The key difference here, of course, is that evaporation leads to significant increases in viscosity of the liquid, leading ultimately to the production of a solid resin film on the substrate.

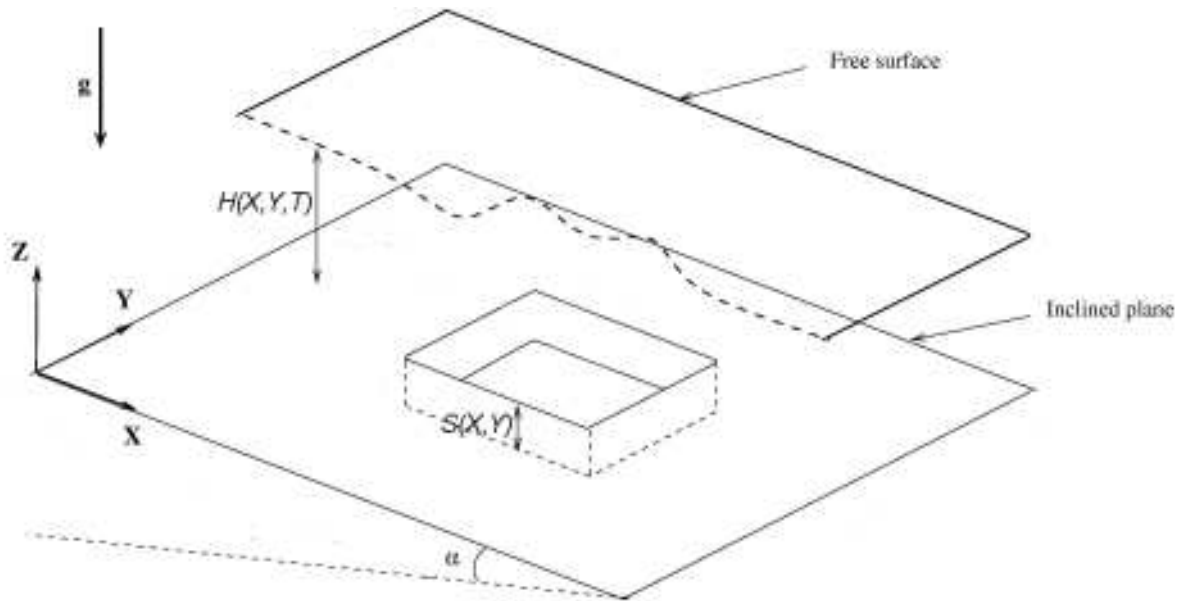


Figure 1: A sketch of a thin film flow down an inclined plate featuring a topography

The assumptions on which the model is based are:

- Inertia effects are negligible, and the ratio ε of the asymptotic film thickness, H_0 , to the characteristic in-plane length scale, L_0 , is small. This means that the flow can be analysed using a lubrication approximation resulting from the long-wave expansion of the Navier-Stokes and continuity equations in terms of ε .

- Marangoni effects can be neglected as the flow is convection-dominated. Hence the surface tension, σ , is taken to be constant and uniform.
- Diffusion of the solvent is sufficiently rapid to ensure a uniform distribution of solvent across the thickness of the film. This is the so-call 'well-mixed' assumption, Howison *et al.* (1997)
- The dynamic viscosity, μ , is assumed to depend exponentially on the solvent concentration, c_s , via the relationship (Schwartz *et al.* 2001),

$$\mu = \mu_0 \exp[a(c_0 - c_s)]$$

where μ_0 is a reference viscosity, c_0 is the initial solvent concentration, and a controls the sensitivity of the viscosity to variations in the concentration.

Under these assumptions, the (dimensionless) governing equations are:

For the film thickness, h :

$$\frac{\partial h}{\partial t} = \frac{\partial}{\partial x} \left[\frac{h^3}{3\tilde{\mu}} \left(\frac{\partial p}{\partial x} - 2 \right) \right] + \frac{\partial}{\partial y} \left[\frac{h^3}{3\tilde{\mu}} \left(\frac{\partial p}{\partial y} \right) \right] - \frac{e}{\varepsilon}$$

For the pressure, p :

$$p = -6\nabla^2 (h + s) + 2^{4/3} Ca^{1/3} \cot \alpha (h + s - z)$$

For the solvent concentration:

$$\frac{\partial c_s}{\partial t} = \frac{\partial}{\partial x} \left[\frac{h^3}{3\tilde{\mu}} \left(\frac{\partial p}{\partial x} - 2 \right) \right] \frac{\partial c_s}{\partial x} + \frac{\partial}{\partial y} \left[\frac{h^3}{3\tilde{\mu}} \left(\frac{\partial p}{\partial y} \right) \right] \frac{\partial c_s}{\partial y} - \frac{e(c_s - 1)}{\varepsilon h}$$

Here t is time, x and y are the in-plane co-ordinates, z is the perpendicular coordinate, $\tilde{\mu} = \mu / \mu_0$, e is the evaporation rate, and $Ca = \mu_0 U_0 / \sigma$ is the capillary number. In generating the above equations, the following length, velocity, pressure and time scales have been used:

$$H_0 = \left(\frac{3\mu_0 Q_0}{\rho g \sin \alpha} \right)^{1/3}, L_0 = \left(\frac{\sigma H_0}{3\rho g \sin \alpha} \right)^{1/3}, U_0 = \frac{3Q_0}{2H_0}, P_0 = \frac{\rho g L_0 \sin \alpha}{2}, T_0 = \frac{L_0}{U_0},$$

where Q_0 is the flow rate, ρ the density and g the gravitational acceleration. Using these scales, the variables are non-dimensionalized as follows:

$$h(x, y, t) = \frac{H}{H_0}, s(x, y) = \frac{S}{H_0}, (x, y) = \frac{(X, Y)}{L_0}, z = \frac{Z}{H_0}, p(x, y, t) = \frac{P}{P_0}, (u, v, \varepsilon w) = \frac{(U, V, W)}{U_0}, t = \frac{T}{T_0}$$

The boundary conditions are:

$$\text{Upstream: } h = 1, \frac{\partial h}{\partial x} = 0, c_s = c_0$$

$$\text{Downstream: } \frac{\partial h}{\partial x} = \frac{\partial p}{\partial x} = 0$$

$$\text{Edges parallel to flow: } \frac{\partial h}{\partial y} = \frac{\partial p}{\partial y} = \frac{\partial c_s}{\partial y} = 0$$

Initially, the free surface is flat and the solvent concentration is uniform and equal to c_0 . The above equations are discretised via a finite difference framework and solved using the efficient and accurate implicit multigrid method of Gaskell *et al.* (2004b). Accordingly, small time steps are avoided when the solution varies only slowly, while the accuracy is controlled throughout the solution process.

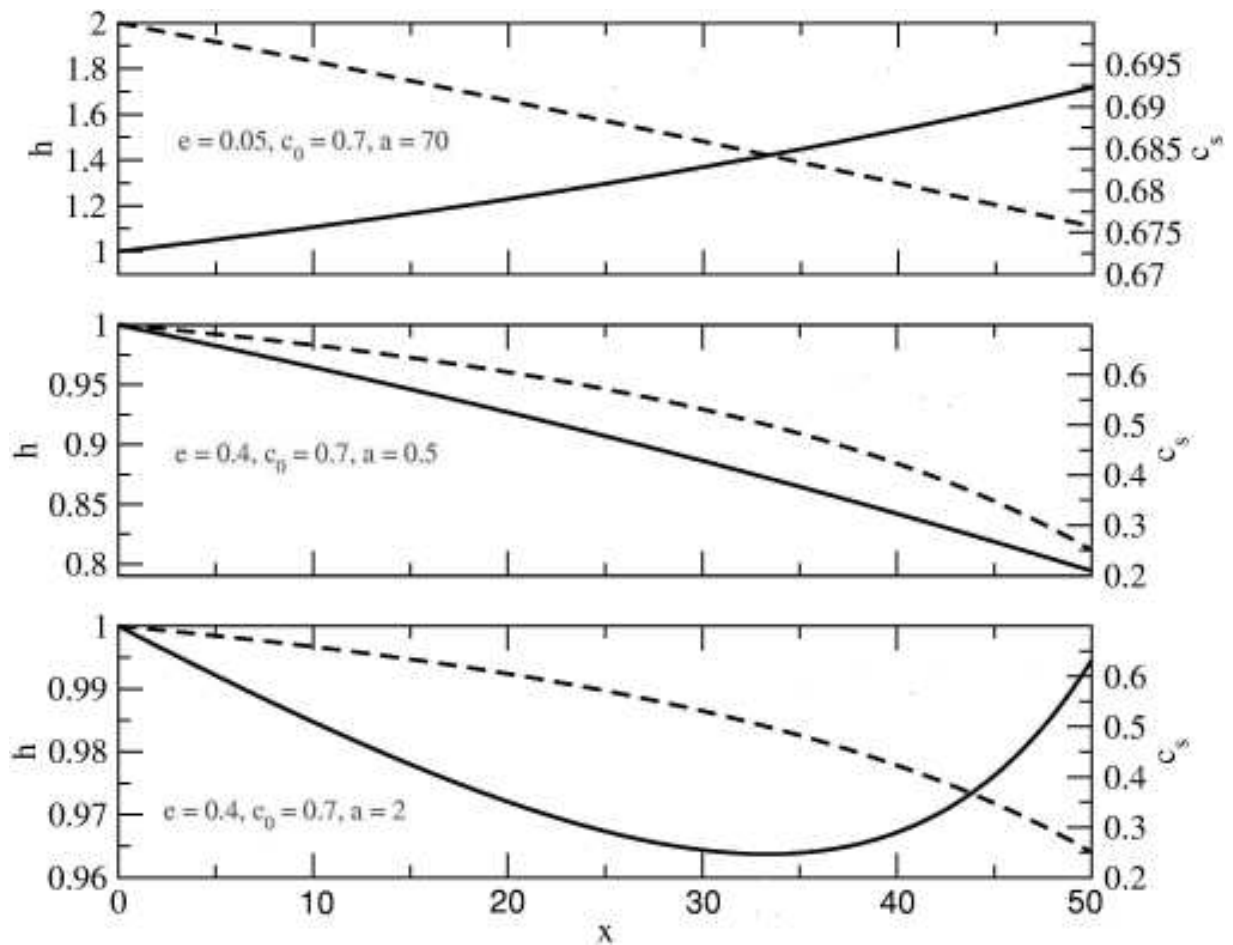


Figure 2: Analytical predictions of film thickness profile (solid lines) and solvent concentration (dashed lines) for a gravity-driven film on a uniform inclined substrate. The asymptotic film thickness was $100\mu\text{m}$, and the inclination angle was 30° .

Results are first presented for the flow of a resin/solvent film down an inclined plane with no topographical features. This is a variation on the problem studied by Huppert (1982), and a simple analytical solution for the film thickness and solvent concentration can be found. This is

useful for testing the numerical formulation of the problem. It is found that three different behaviours are possible, as illustrated in figure 2. For large values of a (the sensitivity parameter), the surface rises due to the increase in viscosity as the solvent evaporates. On the other hand, for small a , the film thins due to solvent loss by evaporation. In intermediate cases, both effects are seen: the film first thins due to solvent loss, but then thickens due to viscosity increases. Time-dependent numerical calculations of the same problem showed excellent agreement with the above results as the simulations approached the steady state.

Adding now a full-width spanwise trench (depth $0.7H_0$ and streamwise width $4L_0$) to the substrate, figure 3 shows the effect of this topography on the film thickness and solvent concentration. Note that the conditions for this simulation are the same as in the uppermost graph in figure 2. Hence one can see that the trench has a marked effect on the film thickness, but does not affect the composition of the resin/solvent mixture or, therefore, the viscosity.

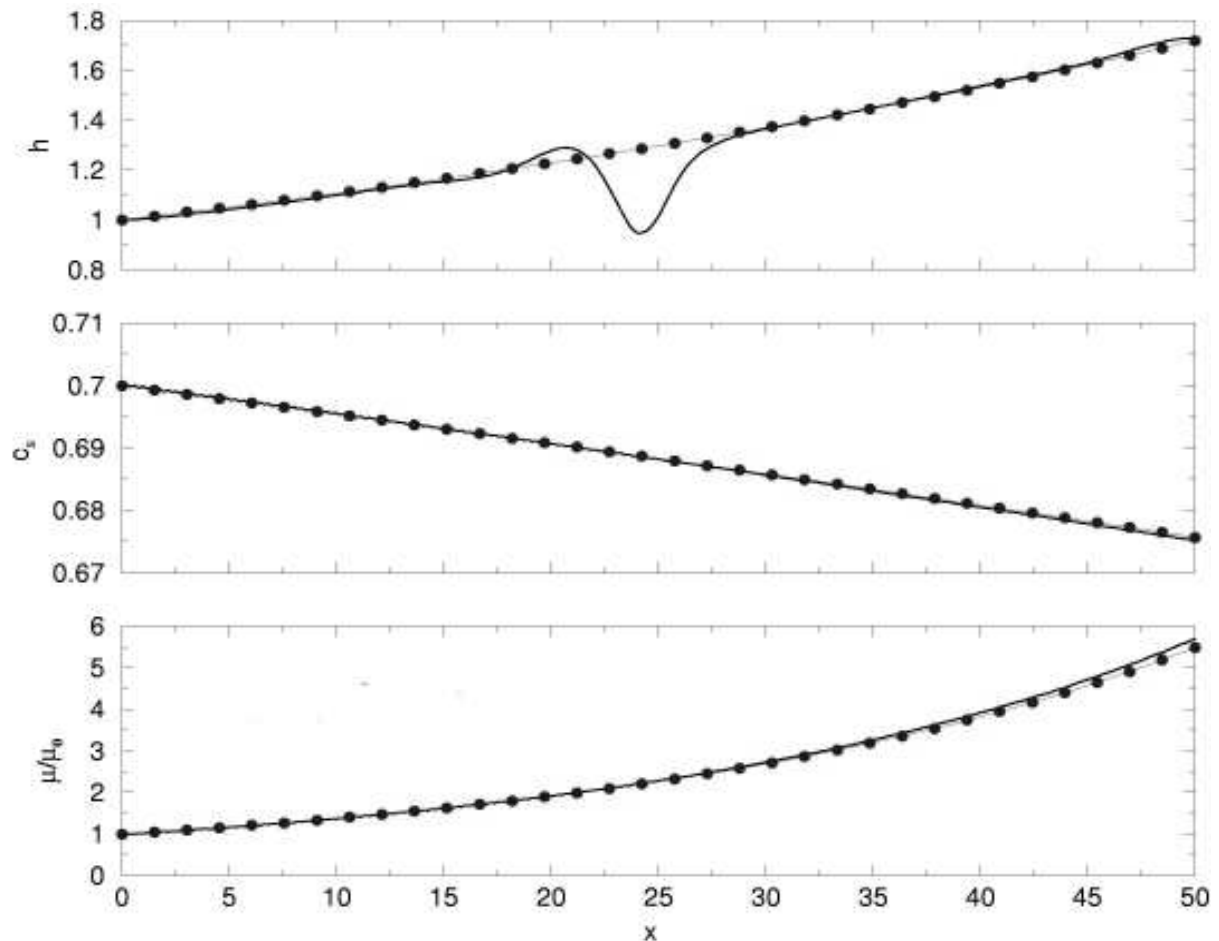


Figure 3: Comparison of steady-state streamwise profiles of film thickness, solvent concentration and viscosity obtained numerically and analytically for flow over a full-width spanwise trench of depth $0.7H_0$ and streamwise width $4L_0$. The solid line is the numerical solution, while the dots are the analytical solution, which neglects the topography.

A very different picture is seen when flow over localized topography is considered. Figure 4 shows 3D views of the free surface and the a surface plot of viscosity which result from flow over a square trench of width 5 capillary lengths and depth H_0 . The free surface view looks similar to that observed by Gaskell *et al.* (2004a) and Decré & Baret (2003) for pure liquids: a curved upstream ridge develops, along with a downstream ‘surge’ in thickness. However, this surface does steadily increase in height downstream, in keeping with the results of figure 3 for the full-width trench. It is in the form of the viscosity (and hence the solvent concentration) that the biggest difference is seen. Figure 4 shows that unlike the full-width trench, the localized trench has a marked and lasting effect on the composition of the resin solution downstream of the topography.

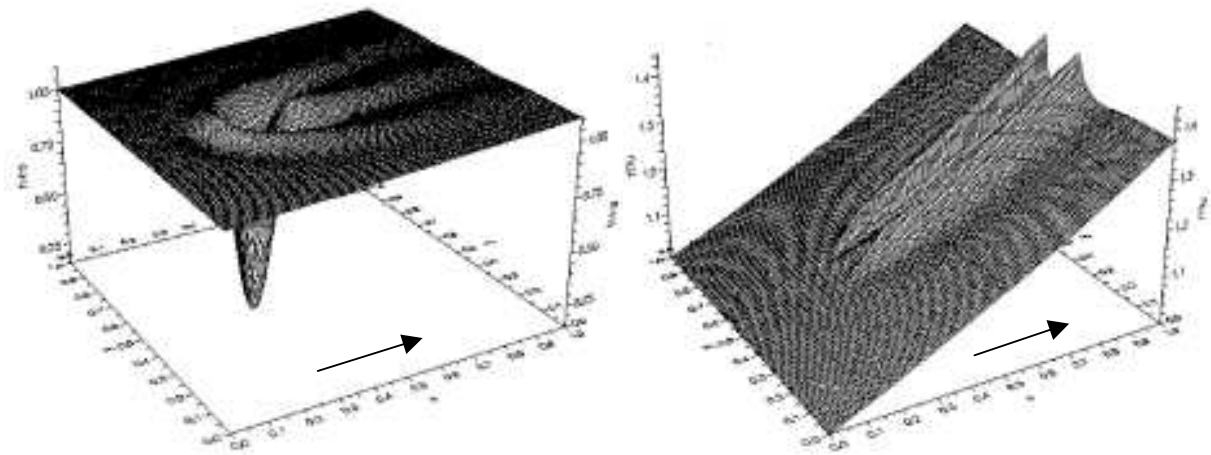


Figure 4: *Left:* a view of the free surface produced in flow over a square trench. *Right:* a corresponding surface plot of viscosity, illustrating the lasting effect of the localized topography. The arrows indicate the direction of flow.

A means of visualizing how a dried film might look is provided by the fictitious ‘resin/solvent interface’, which is defined as $s + (1 - c_s)h$. This ‘interface’, which clearly does not really exist since the resin and solvent are mixed, represents the dried film profile that would be obtained if all the solvent spontaneously evaporated. Figure 5 gives a 3D view of this ‘interface’ for the same flow as depicted in figure 4, and demonstrates the effect of the localized topography on the resulting coated film.

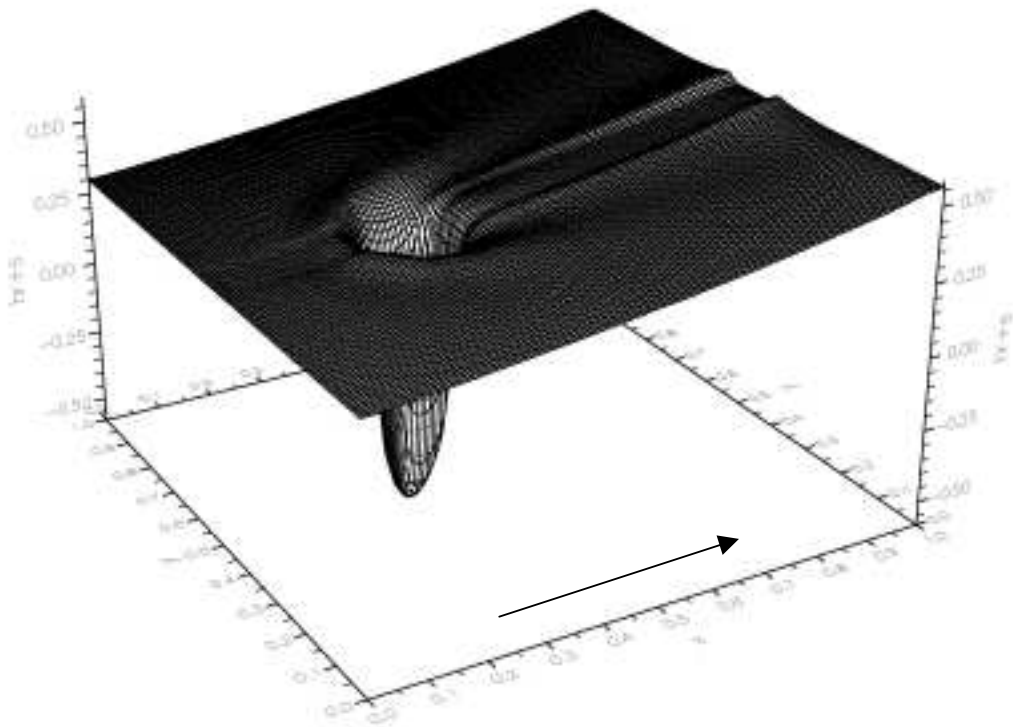


Figure 5: A 3D view of the artificial 'resin/solvent interface', which gives an idea of how the dried film would look if all the solvent spontaneously evaporated. The flow is the same as in figure 4, i.e. that over a square trench. The arrow indicates the direction of flow.

References

- Decré, M.M.J. & Baret, J.-C. (2003) *J. Fluid Mech.* **487**, 147-166.
- Gaskell, P.H., Jimack, P.K., Sellier, M., Thompson, H.M. & Wilson M.C.T. (2004a) *J. Fluid Mech.* **509**, 253-280.
- Gaskell P.H., Jimack P.K., Sellier M. & Thompson H.M. (2004b) *Int. J. Numer. Meth. Fluids*, **45**, 1161-1186.
- Howison, S.D., Moriarty, J.A., Ockendon, J.R., Terrill, E.L. & Wilson, S.K. (1997) *J. Eng. Math.* **32**, 377-394.
- Huppert, H.E. (1982) *Nature* **300**, 427-429.
- Schwartz L.W., Valery Roy R., Eley R.R. & Petrash S. (2001) *J. Coll. Interf. Science*, **234**, 363-374.